IL NUOVO CIMENTO **41 C** (2018) 154
DOI 10.1393/ncc/i2018-18154-0

COLLOQUIA: LaThuile 2018

Search for direct top squark pair production in events with a Higgs or Z boson, and missing transverse momentum in $\sqrt{s} = 13$ TeV pp collisions with the ATLAS detector

G. D'AMEN(1)(2) on behalf of the ATLAS COLLABORATION

(1) *INFN, Sezione di Bologna - Bologna, Italy*
(2) *Dipartimento di Fisica, Università di Bologna - Bologna, Italy*

received 6 September 2018

Summary. — A search for direct top squark pair production resulting in events with either a same-flavour opposite-sign dilepton pair with invariant mass compatible with a Z boson or a pair of jets compatible with a Standard Model (SM) Higgs boson (h) is presented. Requirements on additional leptons, jets, jets identified as originating from b-quarks, and missing transverse momentum are imposed to target the other decay products of the top squark pair. The analysis is performed using proton-proton collision data at $\sqrt{s} = 13$ TeV collected with the ATLAS detector at the LHC in 2015–2016, corresponding to an integrated luminosity of 36.1 fb^{1}. No excess is observed in the data with respect to the SM predictions. The results are interpreted in two sets of models. In the first set, direct production of pairs of lighter top squarks ($\widetilde{t}_1$) with long decay chains involving Z or Higgs bosons is considered. The second set includes direct pair production of the heavier top squark pairs ($\widetilde{t}_2$) decaying via $\widetilde{t}_2 \to Z\,\widetilde{t}_1$ or $\widetilde{t}_2 \to h\,\widetilde{t}_1$. The results exclude at 95% confidence level $\widetilde{t}_2$ and $\widetilde{t}_1$ masses up to about 800 GeV, extending the exclusion region of supersymmetric parameter space covered by previous LHC searches.

1. – Motivations

Searches for supersymmetrical partners of the Standard Model particles have always been one of the main focus of the ATLAS experiment [1], as the confirmation of their existence could potentially explain several inconsistencies between the current description of high-energy physics and experimental data. One major flaw of the current model of particles is the inability to explain the observed value of the Higgs boson mass, leading to the so-called Hierarchy problem; the contribution from particles interacting with the Higgs leads to a quadratic divergence of its mass term in the sole SM hypotesis. As the biggest radiative contribution to the Higgs mass is given by the top quark (due to its high coupling), the supersymmetric partner of the quark top (stop) could be the major

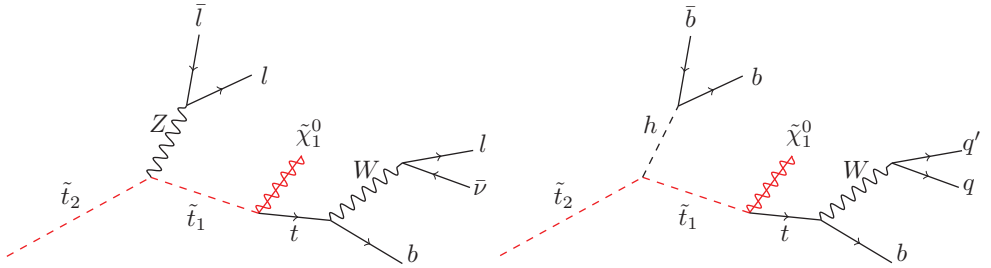

Fig. 1. – Diagrams for the top squark pair production processes considered in this analysis: (a) $\widetilde{t}_2 \to \widetilde{t}_1 Z$ (StopZ branch) and (b) $\widetilde{t}_2 \to \widetilde{t}_1 h$ (StopH branch) [5].

responsible for the cancellation of the quadratic divergence of the Higgs mass [2,3]. The stop squark is also expected to be not too much heavier than the $\mathcal{O}$(TeV), making possible the experimental observation of its production and decay at the LHC experiments [4,6]. The phenomenology of the stop squark takes into account the mixing of the $\widetilde{t}_{L,R}$ (superpartners of the helicity eigentstated of the top quark) in two mass eigenstates, $\widetilde{t}_{1,2}$ with $\widetilde{t}_1$ lighter by convention. Dedicated searches for direct $\widetilde{t}_1$ pair production are common in high-energy physics experiments and are usually optimized for the simplified decay:

$$\widetilde{t}_1 \to \widetilde{\chi}_1^0 + t, \tag{1a}$$

where $\widetilde{\chi}_1^0$ is the lightest neutralino. Targeting complex decay chains requires the introduction of discriminants built from the kinematics of the produced particles. One of the possibilities is to target the decay chain of the heavier $\widetilde{t}_2$ with the production of a Z or Higgs boson:

$$\widetilde{t}_2 \to \widetilde{t}_1 + Z/h \tag{2a}$$

and the subsequent decay of $\widetilde{t}_1$ in $\widetilde{\chi}_1^0$ and a top quark (fig. 1). The search is restricted in a narrow kinematic region where the mass of the $\widetilde{t}_1$ squark equals the mass of its decay products: $m_{\widetilde{t}_1} \simeq m_{\widetilde{\chi}_1^0} + m_t$.

Being the masses of the supersymmetric states unknown, the search targets a grid of signal models with different masses, covering the $\widetilde{t}_2$-$\widetilde{\chi}_1^0$ mass space. The presented study [5] targets the direct pair production of two $\widetilde{t}_2$ and the subsequent decay of each of them in one of two possible simplified decay models [7,8], in either $\widetilde{t}_2 \to \widetilde{t}_1 Z$ (StopZ branch) or $\widetilde{t}_2 \to \widetilde{t}_1 h$ (StopH branch) with branching ratio $\mathcal{B} = 100\%$ each.

2. – StopZ decay branch

2˙1. *Event selection.* – Events of interest are selected if they contain at least three signal leptons (electrons or muons), with at least a pair of leptons, of same flavor and opposite sign, having an invariant mass compatible with a Z boson. The leptons tracks are required to have a p_T over a threshold and to satisfy criteria of quality and isolation.

2˙2. *Signal Region optimization.* – To maximise the sensitivity in different regions of the mass parameter space, three overlapping signal regions (SRs) are defined from the selection criteria defined in table I, where $m^{\ell\ell}$ is the mass of the dilepton pair reconstructed

TABLE I. – *Definition of the signal regions used in the StopZ selection* [5].

Var/region	$\mathrm{SR}_A^{3\ell 1b}$	$\mathrm{SR}_B^{3\ell 1b}$	$\mathrm{SR}_C^{3\ell 1b}$
Number of leptons	≥ 3	≥ 3	≥ 3
n_b*-tagged jets*	≥ 1	≥ 1	≥ 1
$\mid m^{\ell\ell} - m_Z \mid$ [GeV]	< 15	< 15	< 15
Leading lepton p_T [GeV]	> 40	> 40	> 40
Leading jet p_T [GeV]	> 250	> 80	> 60
Leading b-tagged jet p_T [GeV]	> 40	> 40	> 40
$n_{jets}(p_T > 30$ GeV)	≥ 6	≥ 6	≥ 5
E_T^{miss} [GeV]	> 100	> 180	> 140
$p_T^{\ell\ell}$ [GeV]	> 150	–	< 80

as coming from the leptonic decay of the Z boson and $p_T^{\ell\ell}$ its transverse momentum. Signal region $\mathrm{SR}_A^{3\ell 1b}$([1]) is optimised for large $\widetilde{t}_2$-$\widetilde{\chi}_1^0$ mass splitting, where the Z boson in the decay $\widetilde{t}_2 \to \widetilde{t}_1 + Z$ is boosted, and large $p_T^{\ell\ell}$ and leading-jet p_T are required. Signal region $\mathrm{SR}_A^{3\ell 1b}$ covers the intermediate case, featuring slightly softer kinematic requirements than in $\mathrm{SR}_A^{3\ell 1b}$. Signal region $\mathrm{SR}_C^{3\ell 1b}$ is designed to improve the sensitivity for compressed spectra ($m_{\widetilde{t}_2} \gtrsim m_{\widetilde{\chi}_1^0} + m_t + m_Z$) with softer jet p_T requirements and an upper bound on $p_T^{\ell\ell}$.

2˙3. *Standard Model background.* – The main SM background processes satisfying the SR requirements are estimated by Monte Carlo simulation and normalised and verified (whenever possible) with data events in statistically independent regions of the phase space. Dedicated control regions (CRs) enhanced in a particular background component are used for the normalisation. For each SR, a simultaneous background fit is performed to the numbers of events found in the CRs, using a minimisation based on likelihoods. The selections of these CRs are chosen to be the as close as possible (but statistically independent) to the SR selection. Effect due to *fakes and non-prompt leptons* have been estimated with data driven matrix-method. The associated production of a $t\bar{t}$ pair and a Z boson is targeted in the region $\mathrm{CRTZ}^{3\ell 1b}$; an upper cut on $E_T^{miss} < 100$ GeV ensures orthogonality with respect to each SR. The region is enriched in $t\bar{t}+Z$ events, accounting to $\approx 60\%$ of the total. The production of multiple bosons (VV + VVV) is targeted in the region $\mathrm{CRVV}^{3\ell 1b}$; a b-veto ensures orthogonality with respect to each SR. The region is enriched in VV and VVV events, accounting to $\approx 80\%$ of the total.

3. – StopH decay branch

3˙1. *Event selection.* – In the StopH selection, events are selected by a trigger requiring at least four b-tagged jets and one or two leptons, either electrons or muons. This ensures orthogonality with respect to the StopZ selection in case of statistical combination of the two results. At least one lepton is required to have $p_T > 30$ GeV, and the electron candidates are also required to satisfy the tight likelihood-based identification requirement as defined in refs. [9, 10].

3˙2. *Signal Region optimization.* – Similarly to the StopZ case, three overlapping SRs are defined in the StopH selection to improve sensitivity in different regions of the mass

([1]) Where $3\ell 1b$ stands for: selection of three leptons and one b-tagged jet

TABLE II. – *Definition of the signal regions used in the StopH selection* [5].

Requirement/region	$\mathrm{SR}_A^{1\ell 4b}$	$\mathrm{SR}_B^{1\ell 4b}$	$\mathrm{SR}_C^{1\ell 4b}$
Number of Leptons	1–2	1 – 2	1 – 2
n_b-*tagged jets*	≥ 4	≥ 4	≥ 4
m_T [GeV]	–	> 150	> 125
H_T [GeV]	> 1000	–	–
E_T^{miss} [GeV]	> 120	> 150	> 150
Leading b-tagged jet p_T [GeV]	–	–	< 140
m_{bb} [GeV]	95 – 155	–	–
p_T^{bb} [GeV]	> 300	–	–
n_{jet} ($p_T > 60$ GeV)	≥ 6	≥ 5	–
n_{jet} ($p_T > 30$ GeV)	–	–	≥ 7

parameter space. These SRs are defined as shown in table II, where m^{bb} is the mass of the $b\bar{b}$ pair reconstructed as coming from the hadronic decay of the Higgs boson and p_T^{bb} its transverse momentum. Signal region $\mathrm{SR}_A^{1\ell 4b}$([2]) is optimised for large $\widetilde{t}_2 \to \widetilde{\chi}_1^0$ mass splitting, where the Higgs boson in the $\widetilde{t}_2 \to t_1 h$ decay is boosted. In this SR, the pair of b-tagged jets with the smallest ΔR^{bb} is required to have an invariant mass consistent with the Higgs boson mass ($|m_{bb} - m_h| < 15$ GeV, with $m_h = 125$ GeV), and the transverse momentum of the system formed by these two b-tagged jets (p_T^{bb}) is required to be above 300 GeV. Signal region $SR_B^{1\ell 4b}$ covers the intermediate case, featuring slightly harder kinematic requirements than $SR_A^{1\ell 4b}$. Finally, signal region $SR_C^{1\ell 4b}$ is designed to be sensitive to compressed spectra ($m_{\widetilde{t}_2} \gtrsim m_{\widetilde{\chi}_1^0} + m_t + m_h$). This region has softer jet p_T requirements and an upper bound on the p_{T} of the leading b-tagged jet. $SR_A^{1\ell 4b}$ includes requirements on the hadronic activity H_T:

$$H_T = \sum_i \|p_{Ti}\| \tag{3a}$$

for jets with $p_T \geq 30$ GeV. Both SRs $SR_B^{1\ell 4b}$ and $SR_C^{1\ell 4b}$ include requirements on the transverse mass m_T computed using the missing-momentum and lepton-momentum vectors:

$$m_T = \sqrt{2\ p_T^{\ell}\ E_{\mathrm{T}}^{miss}(1 - \cos\Delta\phi(\ell, E_{\mathrm{T}}^{miss}))} \tag{4a}$$

3˙3. *Standard Model background.* – Standard model backgorunds are estimated in the same way as the StopZ case, via a simultaneous background fit in statistically independent CRs. Due to the relatively big differences between the various SRs, multiple CRs are necessary for the normalization of the main background for the StopH case, namely the $t\bar{t}$ pair production. For $\mathrm{SR}_A^{1\ell 4b}$, $\mathrm{SR}_B^{1\ell 4b}$, $\mathrm{SR}_C^{1\ell 4b}$ the background is estimated in $\mathrm{CRT}_A^{1\ell 4b}$, $\mathrm{CRT}_B^{1\ell 4b}$, $\mathrm{CRT}_B^{1\ell 4b}$ respectively. The region is enriched in $t\bar{t}$ events, accounting to $\approx 85\%$ of the total. The statistical independence with respect to the SRs is ensured by inverting the selection on E_{T}^{miss} and by relaxing/inverting the m_T one (table III).

([2]) Where $1\ell 4b$ stands for: selection of one lepton and four b-tagged jet

TABLE III. – *Definition of the control regions used in the StopH selection* [5].

Requirement/Region	$\mathrm{CRT}_A^{1\ell 4b}$	$\mathrm{CRT}_B^{1\ell 4b}$	$\mathrm{CRT}_C^{1\ell 4b}$
Number of Leptons	1 – 2	1 – 2	1 – 2
n_b-*tagged jets*	≥ 4	≥ 4	≥ 4
m_T [GeV]	–	> 100	< 125
E_T^{miss} [GeV]	< 120	< 150	< 150
Leading b-tagged jet p_T [GeV]	–	–	< 140
m_{bb} [GeV]	95 – 155	–	–
p_{bb}^T [GeV]	> 300	–	–
$n_{jets}(p_T > 60$ GeV)	≥ 5	≥ 5	–
$n_{jets}(p_T > 30$ GeV)	–	–	≥ 7

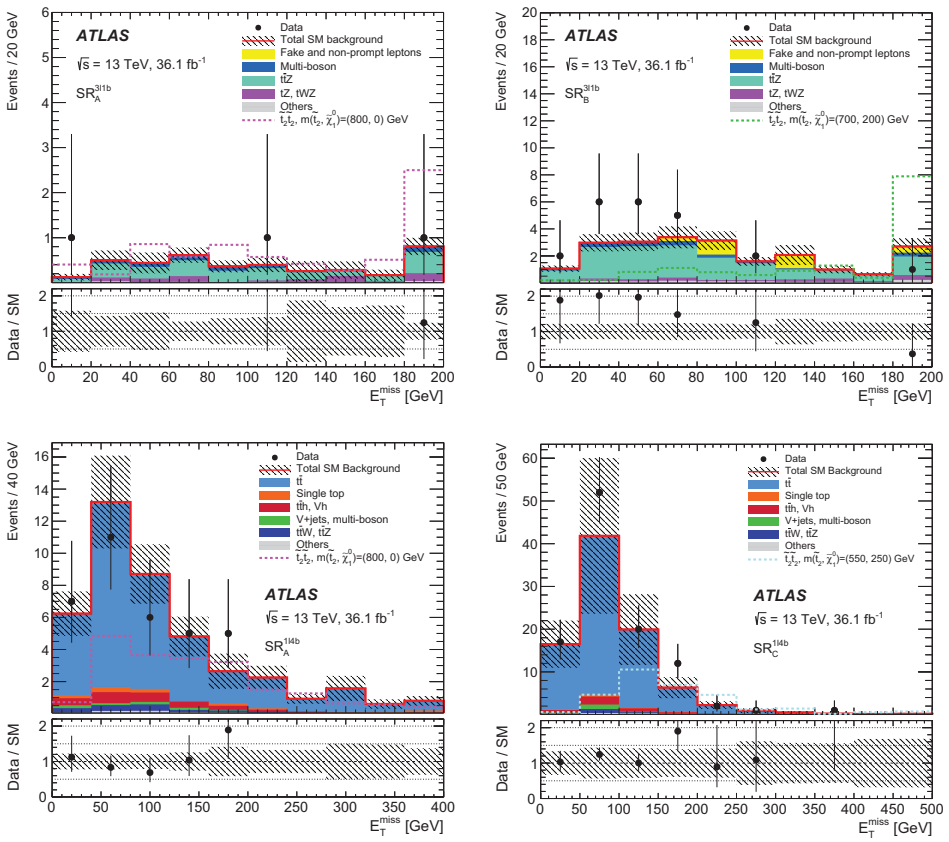

Fig. 2. – Distribution of E_{T}^{miss} (top) and ratio between data and SM predictions (bottom) for events passing all the signal candidate selection requirements, except that on E_{T}^{miss}, for $\mathrm{SR}_A^{3\ell 1b}$ and $\mathrm{SR}_B^{3\ell 1b}$ (top) and $\mathrm{SR}_A^{3\ell 1b}$ and $\mathrm{SR}_B^{3\ell 1b}$ (bottom) after the background fit described before. The lower panels show the ratio of the observed data to the total SM background prediction, with the bands representing the total uncertainty in the background prediction [5].

TABLE IV. – *Observed and expected numbers of events in the three SRs of the StopZ (top) and StopH bottom (branches). The nominal predictions from MC simulation are given for comparison for those backgrounds that are normalised to data in dedicated CRs* [5].

	$SR_A^{3\ell 1b}$	$SR_B^{3\ell 1b}$	$SR_C^{3\ell 1b}$
Observed events	2	1	3
Total (post-fit) SM events	1.9 ± 0.4	2.7 ± 0.6	2.0 ± 0.3
Fit output, multi-boson	0.26 ± 0.08	0.28 ± 0.10	0.23 ± 0.05
Fit input, multi-boson	0.35	0.37	0.30
	$SR_A^{1\ell 4b}$	$SR_B^{1\ell 4b}$	$SR_C^{1\ell 4b}$
Observed events	10	28	16
Total (post-fit) SM events	13.6 ± 3.0	29 ± 5	10.5 ± 3.2
Fit output, $t\bar{t}$	11.3 ± 2.9	24 ± 5	9.3 ± 3.1
Fit input, $t\bar{t}$	7.1	14	6.0

4. – Results

4˙1. *Kinematic distributions and yields.* – Results are evaluated by using a cut-and-count method, by selecting the region of the phase space in which the SUSY signal becomes relevant with respect to the SM background. Distribution of E_{T}^{miss} for events passing all the signal candidate selection requirements, except that on E_{T}^{miss}, for SRs are presented in fig. 2. The contributions from all the SM backgrounds are shown; the grey bands represent the total uncertainty. The expected distributions for signal models with $m(\widetilde{t}_2, \widetilde{\chi}_1^0) = (700, 0)$ GeV, and $m(\widetilde{t}_2, \widetilde{\chi}_1^0) = (650, 250)$ GeV are also shown as dashed lines in the respective SR distribution. The lower panels show the ratio of the observed data to the total SM background prediction, with the bands representing the total uncertainty in the background prediction The observed number of events and expected yields are shown in table IV for each of the six SRs. Data agree with the SM background prediction within uncertainties and thus exclusion limits for several beyond-the-SM (BSM) scenarios are extracted.

4˙2. *Exclusion limits.* – Exclusion limits at 95% CL on the masses of the $\widetilde{t}_2$ and $\widetilde{\chi}_1^0$, for a fixed $m(\widetilde{t}_1) - m(\widetilde{\chi}_1^0) = 180$ GeV and assuming (a) $\mathcal{B}(\widetilde{t}_2 \to \widetilde{t}_1 Z) = 1$ or (b) $\mathcal{B}(\widetilde{t}_2 \to \widetilde{t}_1 h) = 1$ are presented in fig. 3. The dashed line and the shaded band are the expected limit and its $\pm 1\sigma$ uncertainty, respectively. The thick solid line is the observed limit for the central value of the signal cross-section. The expected and observed limits do not include the effect of the theoretical uncertainties in the signal cross-section. The dotted lines show the effect on the observed limit when varying the signal cross-section by $\pm 1\sigma$ of the theoretical uncertainty. The shaded area in the lower-left corner shows the observed exclusion from the ATLAS $\sqrt{s} = 8$ TeV analysis [11].

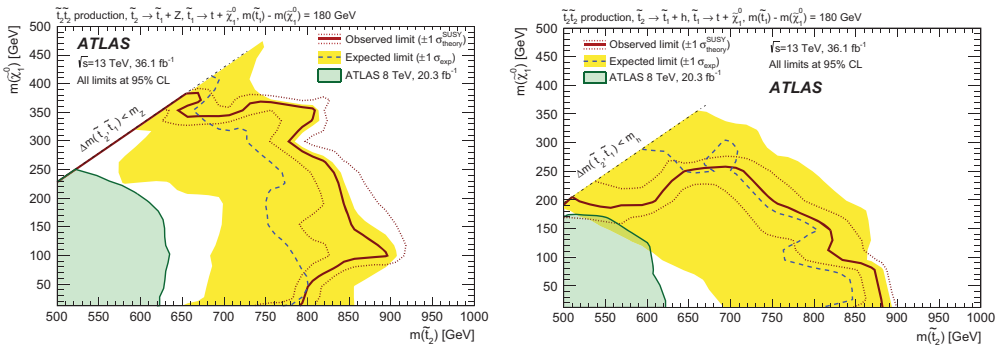

Fig. 3. – Exclusion limits at 95% CL on the masses of the $\widetilde{t}_2$ and $\widetilde{\chi}_1^0$, for a fixed $m(\widetilde{t}_1)$ - $m(\widetilde{\chi}_1^0)$ = 180 GeV and assuming (a) $\mathcal{B}(\widetilde{t}_2 \to \widetilde{t}_1 Z) = 1$ or (b) $\mathcal{B}(\widetilde{t}_2 \to \widetilde{t}_1 h) = 1$ [5].

5. – Stop1 reinterpretation

Results are statistically combined and reinterpreted in a search for $\widetilde{t}_1$ pair production with the same final signature as before:

(5a) $$\widetilde{t}_1 \to \widetilde{\chi}_2^0 t$$

targeting the subsequent decay of the $\widetilde{\chi}_2^0$ in

(6a) $$\widetilde{\chi}_2^0 \to \widetilde{\chi}_1^0 + Z/h.$$

Figure 4 presents exclusion limits at 95% CL from the analysis of 36.1 fb^{-1} of 13 TeV pp collision data on the masses of the $\widetilde{t}_1$ and $\widetilde{\chi}_2^0$, for a fixed $m_{\widetilde{\chi}_1^0}$ = 0 GeV, assuming $\mathcal{B}(\widetilde{\chi}_2^0 \to \widetilde{\chi}_1^0 Z) = 0.5$ and $\mathcal{B}(\widetilde{\chi}_2^0 \to \widetilde{\chi}_1^0 h) = 0.5$. No specific analysis strategy has been applied for this reinterpretation; the two SRs with highest sensitivities from the StopH and StopZ decay branched are statistically combined to derive this limit.

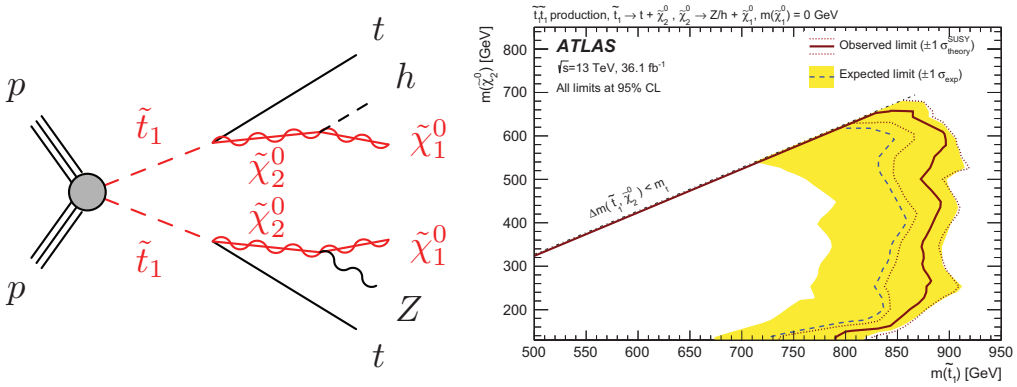

Fig. 4. – Diagrams for the top squark pair production process considered for the Stop1 reinterpretation $\widetilde{t}_1 \to \widetilde{\chi}_2^0 t$ and extracted exclusion limits at 95% CL from the analysis of 36.1 fb^{-1} of 13 TeV pp collision data on the masses of the $\widetilde{t}_1$ and $\widetilde{\chi}_2^0$, for a fixed $m_{\widetilde{\chi}_1^0}$ = 0 GeV, assuming $\mathcal{B}(\widetilde{\chi}_2^0 \to \widetilde{\chi}_1^0 Z) = 0.5$ and $\mathcal{B}(\widetilde{\chi}_2^0 \to \widetilde{\chi}_1^0 h) = 0.5$ [5].

6. – Conclusions

Is presented a search for direct $\widetilde{t}_2$ pair production using pp collision data at $\sqrt{s} =$ 13 TeV collected with the ATLAS detector at the LHC in 2015–2016, corresponding to an integrated luminosity of 36.1 fb[1]. This search targets the decay $\widetilde{t}_2 \to \widetilde{t}_1 + Z/h$ with 100% BR, aiming to study the kinematic region where $m_{\widetilde{t}_1} = m_{\widetilde{\chi}^0_1} + m_t$. Three SRs have been defined for each of the two decay branches, based on the mass splitting between $\widetilde{t}_2$ and $\widetilde{t}_1$. Data agree with the SM background expectation within uncertainties for both the StopZ and StopH decay branches and thus exclusion limits for new physics beyond the SM are extracted, up to ~ 850 GeV for the mass of the $\widetilde{t}_2$ and $\sim 250\,\text{GeV}$ for the mass of the $\widetilde{\chi}^0_1$. Exclusion limits have been statistically combined and reinterpreted for the decay $\widetilde{t}_1 \to \widetilde{\chi}^0_2 + t$, covering masses up to $\sim 900\,\text{GeV}$.

REFERENCES

[1] ATLAS Collaboration, *JINST*, **3** (2008) S08003.
[2] Dimopoulos S., Raby S. and Wilczek F., *Phys. Rev. D*, **24** (1981) 1681.
[3] Sakai N., *Z.Phys. C*, **11** (1981) 153.
[4] Inoue K., Kakuto A., Komatsu H. and Takeshita S., *Prog. Theor. Phys.*, **68** (1982) 927.
[5] ATLAS Collaboration, *JHEP*, **08** (2017) 006.
[6] Ellis J. R. and Rudaz S., *Phys. Lett. B*, **128** (1983) 248.
[7] Alwall J., Schuster P. and Toro N., *Phys. Rev. D*, **69** (2009) 075020.
[8] Alves D. *et al.*, *J. Phys. G*, **39** (2012) 105005.
[9] ATLAS Collaboration, *Eur. Phys. J. C*, **77** (2017) 195.
[10] ATLAS Collaboration, *Electron identification measurements in ATLAS using* $\sqrt{s} =$ 13 *TeV data with 50 ns bunch spacing*, ATL-PHYS-PUB-2015-041 (2015).
[11] ATLAS Collaboration, *Eur.Phys. J. C*, **75** (2015) 510.